Polyadenylic·Polyxanthylic·Polyuridylic Acid Triple Helix†

Paul F. Torrence* and Erik De Clercq*

ABSTRACT: Poly(xanthylic acid) [(X)*n*] abolished the ability of (A)*n*·(U)*n* to induce interferon in "superinduced" (actinomycin D and cycloheximide) primary rabbit kidney cells. Under the same conditions, (X)*n* had a relatively minor effect on the interferon inducing capacity of (I)*n*·(C)*n*. Evidence based on mixing curves, melting profiles, pancreatic ribonuclease resistance and sucrose gradient ultracentrifugation pointed to the conclusion that the following three reactions occur depending on stoichiometry: (1) 2(A)*n*·(U)*n* + (X)*n* → (A)*n*·2(U)*n* + (A)*n*·(X)*n*; (2) (A)*n*·(U)*n* + (X)*n* → (A)*n*·(U)*n*·(X)*n*; (3) (A)*n*·(U)*n* + 2(X)*n* → (A)*n*·(X)*n* + (X)*n*·(U)*n*. The second reaction represents the formation of a new triple helix which can also be formed according to the following reactions: (X)*n*·(U)*n* + (A)*n* → (A)*n*·(X)*n*·(U)*n*; (A)*n*·(X)*n* + (U)*n* → (A)*n*·(X)*n*·(U)*n*.

Interferon induction is exquisitely sensitive to the structural nature of a polynucleotide (e.g., De Clercq, 1974; Torrence et al., 1976). For instance, single- and triple-stranded nucleic acids fail to induce interferon, whereas double-stranded nucleic acids are the most potent inducers known. This sensitivity of the interferon system has been used to monitor a variety of polynucleotide interactions, including triple-helix formation (De Clercq et al., 1975b; Torrence et al., 1976) and displacement reactions (De Clercq et al., 1976). Such studies take on interest for two distinct reasons. Given that a nucleic acid is able to abolish the interferon-inducing capacity of a nucleic acid, the reason for this inhibitory effect may be due to (a) interaction with the inducing molecule itself or (b) interaction with a cellular component(s). In the former instance, a nucleic acid–nucleic acid interaction can be defined that may help to define the role of such interaction in biological systems. In the latter instance, a tool may be provided to gain access to knowledge of the fundamental cellular events involved in the induction process.

In this paper, we show that poly(xanthylic acid) [(X)*n*][1] inhibits the induction of interferon by (A)*n*·(U)*n* and that this inhibition can be explained by the interaction of (X)*n* with (A)*n*·(U)*n* to form the heretofore unrecognized (A)*n*·(X)*n*·(U)*n* triple helix.

Materials and Methods

Techniques used for the determination of interferon production in "superinduced" primary rabbit kidney cells, as well as for the determination of melting profiles and mixing curves, pancreatic RNase A resistance, and sucrose gradient ultracentrifugation, were the same as previously described (De Clercq et al., 1975b). Poly(A) (s_{20} = 7.2) and poly(U) (s_{20} = 6.1) were from P-L Biochemicals. Poly(X) was obtained from two different sources: P-L Biochemicals (s_{20} = 4.5 and 8.2) and Miles Laboratories (s_{20} = 4.7). Both samples behaved the same in regard to melting behavior as single strands or in complexes with complementary polynucleotides. A quadruplicate determination of the extinction coefficient of poly(X) gave ϵ_{max} = 9000 ± 50 (0.10 M NaCl–0.01 M sodium cacodylate, pH 7.0, T = 20 °C). The other ϵ values employed herein were: (A)*n*, ϵ_{max} = 10 000 (Sigler et al., 1962); (U)*n*, ϵ_{max} = 9430 (Blake et al., 1967).

Radiolabeled [8-^{14}C]-(A)*n* and [5-^{3}H]-(U)*n* were obtained from Miles Laboratories (Elkhart, Indiana), diluted with cold polymer to 2 × 10^5 dpm/μmol for [8-^{14}C]-(A)*n* and 2.5 × 10^6 dpm/μmol for 5-[^{3}H]-(U)*n* and then further purified on Sephadex G-100 (2 × 25 cm, 0.04 NH_4Cl, pH 7). Only the material that eluted in the void volume was used in the labeling experiments.

Results and Discussion

The results presented in Table I show that the well-established interferon inducers (A)*n*·(U)*n* and (I)*n*·(C)*n* led to high titers of interferon in the actinomycin D–cycloheximide "superinduced" primary rabbit kidney cell assay. Also, as previously established (De Clercq and Merigan, 1969; Torrence et al., in press), (A)*n*·(X)*n* and (U)*n*·(X)*n* failed to induce interferon. When (X)*n* was mixed in an equimolar amount with (A)*n*·(U)*n*, there resulted a total loss of the ability of (A)*n*·(U)*n* to induce interferon. Furthermore mixtures of the same overall composition, but differently constructed [i.e., (U)*n*·(X)*n* + (A)*n*, (A)*n*·(X)*n* + (U)*n*, or (A)*n* + (U)*n* + (X)*n*], also failed to produce any interferon. (A)*n*·(U)*n*, an active inducer, did not affect the titer of (I)*n*·(C)*n*, but (X)*n*, (A)*n*·(X)*n*, and (U)*n*·(X)*n* as well as differently constructed mixtures of (A)*n*, (U)*n*, and (X)*n* caused a small (three- to tenfold) reduction in (I)*n*·(C)*n*'s interferon titer.

Since (X)*n* caused a profound reduction in the titer of (A)*n*·(U)*n* but had comparatively little effect on the titer of (I)*n*·(C)*n* and since various mixtures of (A)*n*, (U)*n*, and/or (X)*n* had relatively little effect on the titer of (I)*n*·(C)*n*, it was reasonable to assume (if the interferon induction receptor sites for (A)*n*·(U)*n* and (I)*n*·(C)*n* are the same) that the ability of (X)*n* to abolish the titer of (A)*n*·(U)*n* is due to some prior interaction of (X)*n* with (A)*n*·(U)*n* rather than some undefined

† From the Laboratory of Chemistry, National Institutes of Arthritis, Metabolism and Digestive Diseases, United States National Institutes of Health, Bethesda, Maryland 20014 (P.F.T.), and The Rega Institute, Catholic University of Leuven, B-3000 Leuven, Belgium (E.D.C.). *Received September 28, 1976.* This work was supported in part by grants from the Belgian Fonds voor Geneeskundig Wetenschappelijk Onderzoek and the Fonds Derde Cyclus, Katholieke Universiteit te Leuven.

[1] Abbreviations used: polynucleotides are abbreviated according to the standard manner: e.g., (X)*n*, poly(xanthylic acid); (A)*n*, poly(adenylic acid); (U)*n*, poly(uridylic acid); (I)*n*, poly(inosinic acid); (C)*n*, poly(cytidylic acid). Other abbreviations include: MEM, Eagle's minimal essential medium; Hepes, *N*-2-hydroxyethylpiperazine-*N'*-2-ethanesulfonic acid.

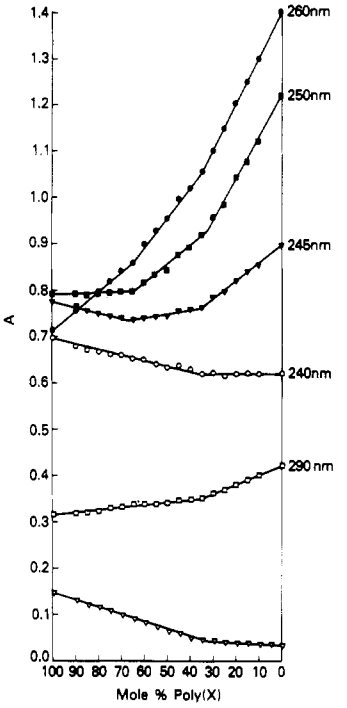

FIGURE 1: Mixing curve (continuous variation method) for the interaction of (X)n with (A)n·(U)n in 0.10 M NaCl–0.01 M sodium cacodylate, pH 7, T = 20 °C. Absorbancies were determined 48 h after mixing and remained constant when redetermined 1 week later: (●) 260 mm; (■) 250 mn; (▼) 245 nm; (○) 240 nm; (□) 290 nm; (▽) 295 nm; 50 mol% (X)n refers to a ratio of 1 mol of (X)n to 1 mol of duplex or 1 mol of (X)n P to 2 mol of duplex P.

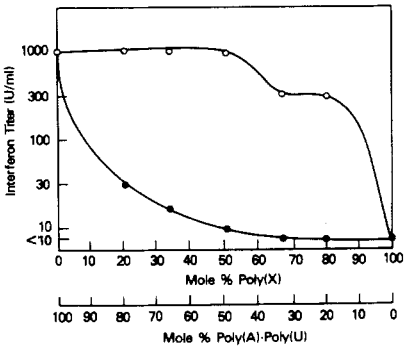

FIGURE 2: "Interferon mixing curve" representing the variation of interferon titer [in "superinduced" (actinomycin D and cycloheximide) primary rabbit kidney cells] according to the mol % of (X)n in a mixture with (A)n·(U)n. Different mixtures of (A)n·(U)n and (X)n were incubated together at 37 °C for 1 h in MEM before application to the cells. The upper curve (○) represents the effect of decreasing concentrations of (A)n·(U)n. The lower curve (●) represents the interferon titer for (A)n·(U)n + (X)n mixture of varying composition.

inhibition of interferon production at the cellular level. The following possibilities may be entertained:

(1) triplex formation:

$$(X)n + (A)n\cdot(U)n \rightarrow (X)n\cdot(A)n\cdot(U)n \quad \text{(i)}$$

(2) strand displacement:

$$(X)n + (A)n\cdot(U)n \rightarrow (A)n + (U)n\cdot(X)n \quad \text{(ii)}$$

$$2(X)n + (A)n\cdot(U)n \rightarrow (A)n\cdot(X)n + (U)n\cdot(X)n \quad \text{(iii)}$$

$$(X)n + (A)n\cdot(U)n \rightarrow (U)n + (A)n\cdot(X)n \quad \text{(iv)}$$

TABLE I: The Effect of (X)n and Its Complexes On Interferon Induction by (A)n·(U)n and (I)n·(C)n.

Polynucleotide Mixture[a]	Rel Interferon Titer[b]
(A)n·(U)n	1.0
(I)n·(C)n	3.0–6.0
(U)n·(X)n	<0.01
(A)n·(X)n	<0.01
(A)n·(U)n + (X)n	<0.01
(U)n·(X)n + (A)n	<0.01
(A)n·(X)n + (U)n	<0.01
(A)n + (U)n + (X)n	<0.01
(A)n·(U)n + (I)n·(C)n	3.0–6.0
(U)n·(X)n + (I)n·(C)n	1.5–2.0
(A)n·(X)n + (I)n·(C)n	0.3–0.6
(I)n·(C)n + (X)n	1.0–2.0
(I)n·(C)n + (A)n·(U)n + (X)n	0.6–1.0
(I)n·(C)n + (U)n·(X)n + (A)n	0.6–1.0
(I)n·(C)n + (A)n·(X)n + (U)n	1.0–1.5
(I)n·(C)n + (A)n + (X)n + (U)n	2.0–6.0

[a] Polynucleotide duplexes (e.g., (A)n·(U)n) were constructed from the individual homopolymers at 10^{-4} M in 0.05 M NaCl–0.05 M Hepes, pH 7, buffer and allowed to equilibrate at 4 °C for at least 1 week before determination of interferon titer. The (X)n containing mixtures were prepared under the same conditions. For determination of the effect of such admixtures on the interferon titer of (I)n·(C)n, the samples were incubated together with (I)n·(C)n for 1 h at 37 °C in MEM prior to exposure to the cells. The concentration applied to the cells in all cases was 2.5×10^{-5} M in duplex (5×10^{-5} M in P) and/or 2.5×10^{-5} M in homopolymer (2.5×10^{-5} M in P). [b] Compared with (A)n·(U)n which titered ca. 1000 international units/mL in this representative assay. Interferon titers were determined as described previously (De Clercq et al., 1975b). These titer determinations have been repeated several times with different preparations of primary rabbit kidney cells to give the same orders of reduction of interferon titers.

(3) strand displacement and triplex formation:

$$(X)n + 2(A)n\cdot(U)n \rightarrow (A)n\cdot2(U)n + (A)n\cdot(X)n \quad \text{(v)}$$

$$2(X)n + 2(A)n\cdot(U)n \rightarrow (A)n\cdot2(U)n + (A)n\cdot2(X)n \quad \text{(vi)}$$

$$3(X)n + (A)n\cdot(U)n \rightarrow (A)n\cdot2(X)n + (U)n\cdot(X)n \quad \text{(vii)}$$

$$2(X)n + (A)n\cdot(U)n \rightarrow (U)n + (A)n\cdot2(X)n \quad \text{(viii)}$$

To determine whether or not (X)n could interact with (A)n·(U)n, a mixing curve was constructed using the method of continuous variations. The result, shown in Figure 1, clearly indicated that (X)n does interact with (A)n·(U)n and that in fact two different reactions occur, one with the stoichiometry of 2(X)n/1(A)n·(U)n, and a second reaction with a ratio of (X)n/(A)n·(U)n of 1:2. To determine if this result had any correspondence with the in vitro tissue culture situation, an "interferon mixing curve" (Figure 2) was constructed using various mole percentage mixtures of (A)n·(U)n and (X)n. Remarkably, the "interferon mixing curve" corresponded to the stoichiometry of the first reaction; that is, the break occurred at a ratio of (X)n/(A)·(U)n of 1:2. The other breaks in the spectrophotometric mixing curve are not reflected in the interferon experiment since none of the remaining products are capable of inducing interferon (vide infra).

The nature of the (X)n + (A)n·(U)n reaction products was determined in the following way:

(1) Melting profiles were determined for (X)n–(A)n·(U) mixtures corresponding to the two stoichiometries indicated

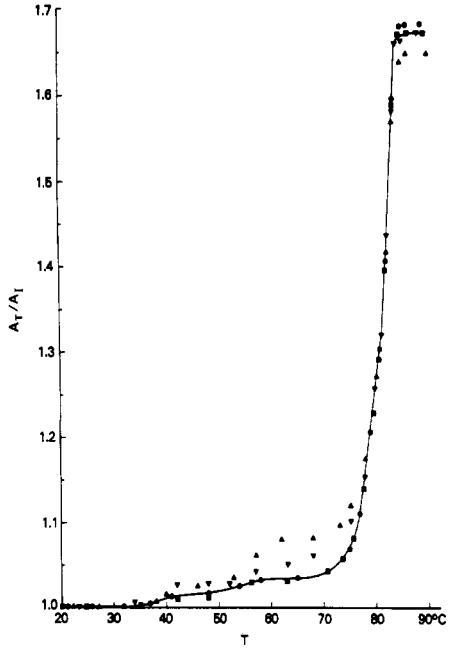

FIGURE 3: Ultraviolet absorbance–temperature profile for the following (all in 0.10 M NaCl–0.01 M sodium cacodylate, pH 7.0): (A)n + (X)n + (U)n (▼); (A)n·(U)n + (X)n (▲); (A)n·(X)n + (U)n (■); (U)n·(X)n + (A)n (●). T_m's were determined 1 week after mixing. No other transitions were revealed by monitoring other wavelengths (e.g., 290, 280, 270, 250 nm).

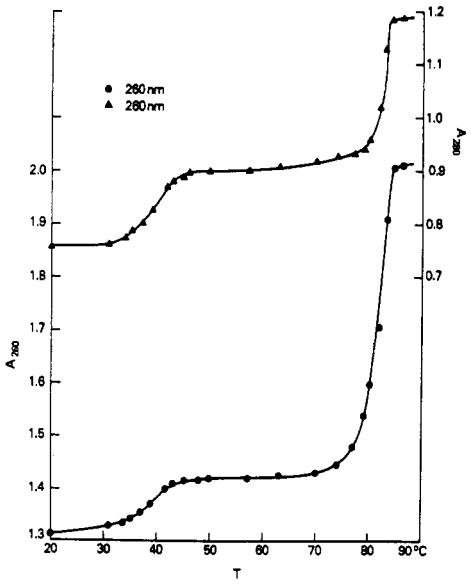

FIGURE 4: A melting profile for the mixture (A)n·(U)n + 2(X)n. In addition, mixtures constructed from (A)n·2(X)n + (U)n and (A)n·(X)n + (X)n·(U)n gave rise to the identical profile (all determined in 0.10 M NaCl–0.01 M sodium cacodylate, pH 7.0): (●) 260 min; (■) 280 nm.

in the mixing curve as well as a 50 mol % mixture. The 1:1 mixture melted monophasically (Figure 3) but the 1(A)n·(U)n/2(X)n (Figure 4) and 2(A)n·(U)n/1(X)n (data not shown) mixtures melted in two steps. In all three instances, the final transition occurred at T_m 80–82 °C corresponding to the value determined under the same conditions for the (A)n·(X)n duplex/or (A)n·2(X)n triplex (Fikus and Shugar, 1969; Michelson and Monny, 1966; Torrence et al., in press). The mixture 2(A)n·(U)n/1(X)n (not shown) showed a first transition at T_m 57 °C corresponding to the melting of (A)n·(U)n

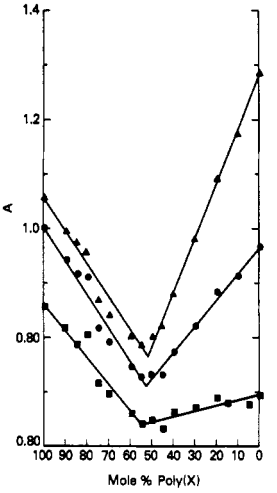

FIGURE 5: Mixing curve (continuous variations) for the interaction of (A)n·(U)n + (X)n at T = 48 °C in 0.10 M NaCl–0.01 M sodium cacodylate, pH 7. The mixtures were allowed to equilibrate for 1 week at ambient temperature before the absorbancies were determined: (●) 245 nm; (▲) 250 nm; (■) 240 nm. Other monitored wavelengths showed the same behavior. See Figure 1 for other details.

or (A)n·2(U)n. Since this mixture did not induce interferon, the presence of (A)n·(U)n can be excluded so that the following reaction must occur.

$$2(A)n\cdot(U)n + (X)n \rightarrow (A)n\cdot(X)n + (A)n\cdot 2(U)n \quad \text{(ix)}$$

The lower melting transition (T_m ~39 °C) of the mixture 1(A)n·(U)n/2(X)n (Figure 4) did not exactly correspond to any of the possible products of the reaction but comes closest to the melting of (U)n·(X)n (T_m = 42 °C). The transition is also less cooperative than would be expected for (U)n·(X)n. This transition will be discussed in more detail below.

To attempt to simplify the nature of the (A)n·(U)n + (X)n reaction, a mixing curve was constructed in the same buffer but at 48 °C which is the plateau region in the melting profile of the 2(X)n/1(A)n·(U)n (Figure 4) mixture. Thus, at least that particular reaction should be eliminated. In this instance (Figure 5), the results were unambiguous and showed a 1:1 stoichiometry with no evidence for any other reaction. While the reaction with stoichiometry 2(X)n/1(A)n·(U)n should have been eliminated (since the temperature was above the first transition in its melting profile), the reaction with stoichiometry 2(A)n·(U)/1(X)n should not have been. It is possible that this second reaction may still occur, but the nature of the mixing curve may make it invisible. Alternatively, an inversion of stabilities may have occurred.

Since these data implied that (A)n·(U)n + (X)n also did react with 1:1 stoichiometry, alternate pathways to the same unknown structure were investigated; namely, the interaction of (A)n·(X)n + (U)n and the interaction of (U)n·(X)n + (A)n. Neither of these two combinations was capable of inducing interferon (Table I). Mixing curves were constructed at various wavelengths for both these systems and the results for one system are given in Figure 6. It is clear that (A)n·(X)n reacts with (U)n in 1:1 stoichiometry and that (U)n·(X)n reacts with (A)n in 1:1 stoichiometry. There was no evidence for interactions at other stoichiometries in either instance.

In concert with the mixing curve data, melting profiles for the interactions (A)n·(U)n + (X)n, (U)n·(X)n + (A)n, (A)n·(X)n + (U)n, and (A)n + (X)n + (U)n were identical (Figure 3). Thus all four reaction pathways appear to lead (at equilibrium) to the same product. Other melting profile data

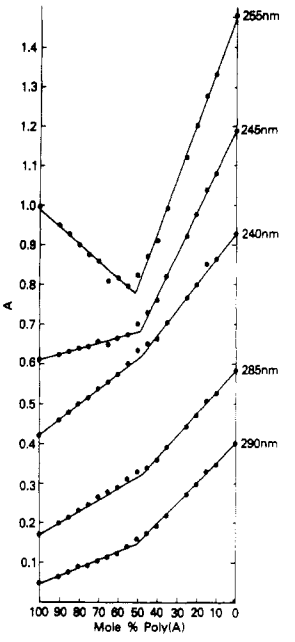

FIGURE 6: Mixing curve for the interaction of (A)n + (X)n·(U)n in 0.01 M NaCl–0.01 M sodium cacodylate, pH 7, T = 20 °C. Constructed using the same protocol as in Figure 1; 50 mol % (A)n refers to 1 mol of (A)n/1 mol of duplex or 1 mol of (A)n P to 2 mol of duplex P.

in equimolar mixtures of (A)n + (U)n + (X)n failed to reveal the presence of either free (U)n (T_m 8 °C in 0.01 M $MgCl_2$) or free (X)n (T_m 30 °C in 0.10 M NaCl, pH 7). The presence of free (A)n could also be eliminated since free (A)n would give rise to a substantial noncooperative temperature-dependent hyperchromicity before the major transition (Figure 3).

Further information regarding the nature of the (A)n·(U)n + (X)n reaction product was gathered from pancreatic RNase A resistance experiments (data not shown). As expected, labeled (U)n was rapidly degraded by RNase A but, when combined with (A)n to give the (A)n·(U)n duplex, the label became quite resistant to solubilization. The addition of a second mole of labeled (U)n to (A)n·(U)n gives the triple-helical complex (A)·2(U)n and the label in this form was also highly resistant to degradation by RNase A. That free (U)n could reasonably be expected to be detected under such conditions was shown by the addition of yet another mole of labeled (U)n to the (A)n·2(U)n triplex. That addition resulted in a significant (⅓) drop in resistance of the label to degradation due to the presence of free (U)n. When cold (X)n was added to (A)n·(U)n (with the (U)n labeled), there was no drop in resistance of the (U)n to degradation as compared with (A)n·(U)n. In fact, there was a significant increase in resistance. This experiment corroborates the results of the melting profile experiments and demonstrates that in an equimolar mixture of (A)n·(U)n + (X)n there is no free (U)n.

Sucrose gradient ultracentrifugation experiments (Figures 7a and 7b) also corroborated and extended the above findings. (a) [^{14}C]-(A)n alone peaked at fractions 10–11 and [^{14}C]-(A)n·(U)n peaked at fractions 17–18. When (X)n was added to the [^{14}C]-(A)n·(U)n, the product banded at fractions 17–22, thus eliminating free (A)n as a product of the reaction (Figure 7a). (b) Similarly, [5-^{3}H]-(U)n peaked at fraction 8, while [5-^{3}H]-(U)n·(A)n peaked at fractions 14–15 and [5-^{3}H]-(U)n·(X)n peaked at fraction 13. When cold (X)n was mixed with [5-^{3}H]-(U)n·(A)n, the product banded at fractions 13–25 with no evidence for the release of free (U)n (Figure 7b).

To summarize, the interactions (A)n·(U)n + (X)n,

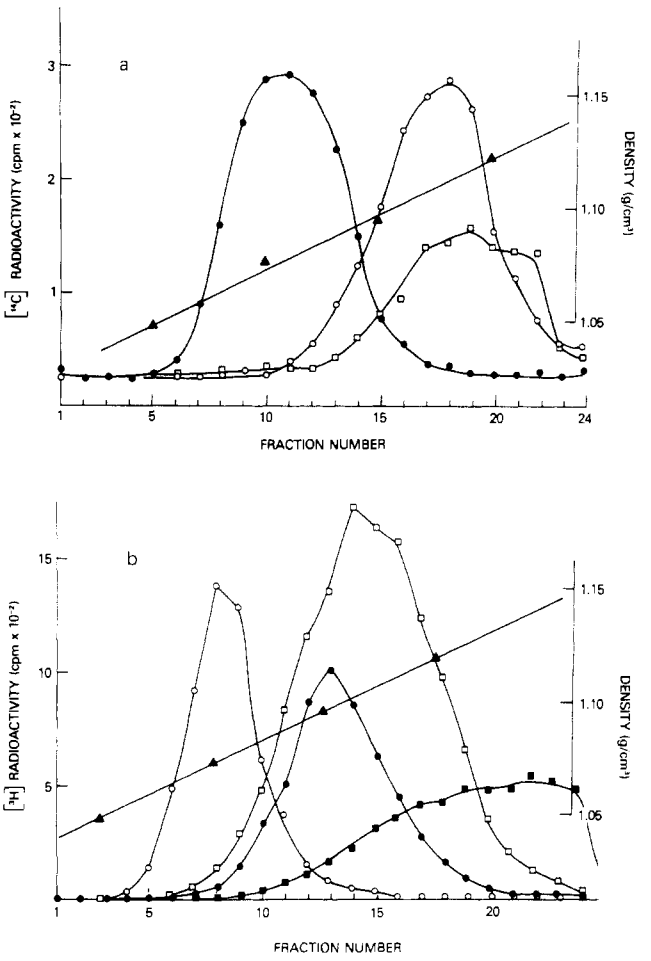

FIGURE 7: (a) Sucrose gradient ultracentrifugation profile for [^{14}C](A)n (●), [^{14}C](A)n·(U)n (○), and [^{14}C](A)n·(U)n + (X)n (□). (b) Same but for [^{3}H](U)n (○), [^{3}H](U)n·(X)n (●), [^{3}H](A)n (□), and [^{3}H](U)n·(A)n + (X)n (■).

(A)n·(X)n + (U)n, and (X)n·(U)n + (A)n can all occur with 1:1 stoichiometry and all three interactions (as well as an equimolar mixture of (A)n + (X)n + (U)n) give rise to the same melting profile that shows no evidence for free (X)n, (A)n, (U)n, (A)n·(U)n, or (X)n·(U)n. In addition, pancreatic RNase A resistance experiments and sucrose gradient ultracentrifugation show the absence of both free (U)n and free (A)n in equimolar mixtures of (A)n, (U)n, and (X)n. In light of these experiments, reaction possibilities ii–viii can be eliminated and the common reaction product must be a triply stranded complex (A)n·(X)n·(U)n. The melting profile in Figure 3 shows but one transition (in 0.10 M NaCl–0.01 M sodium cacodylate, pH 7), but when the ionic strength is lowered (to 0.05 M NaCl–0.01 M sodium cacodylate, pH 7) (not shown), a biphasic transition occurs which most probably represents strandwise melting (3 → 2, 2 → 1) of the triplex. This would imply that the (U)n strand melts off first under these conditions leaving the intact (A)n·(X)n duplex.

A number of reasonable hydrogen-bonding schemes can be formulated for such a triple helix and one possiblity is shown in Figure 8. It is based on the postulated structure of the (A)n·(X)n type duplex (Michelson and Monny, 1966; Fikus and Shugar, 1969) coupled with the strandwise melting behavior witnessed above. In analogy to the (A)·2(U)n situation, the "Hoogsteen" bonded polymer of the triplex melts out first. Similar reasoning was used to assign the structure of the

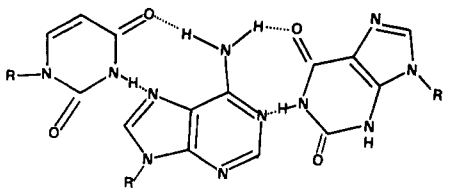

FIGURE 8: A possible formulation of the (A)*n*·(X)*n*·(U)*n* triple helix.

(A)*n*·(U)*n*·(I)*n* triplex (De Clercq et al., 1975b). A final determination must await x-ray fiber diffraction analysis of this triple helix.

Having established the probable existence of the (A)*n*·(U)*n*·(X)*n* triplex, the melting profile for the interaction 1(A)*n*·(U)*n*/2(X)*n* (Figure 4) may be more readily interpreted. It is noteworthy that this same melting profile was obtained for the interaction (A)*n*·(X)*n* + (X)*n*·(U)*n* and (A)*n*·2(X)*n* + (U)*n* indicating that all three reactions give the same (noninterferon inducing) product. It seems most likely that the lower, rather broad transition (T_m ~38 °C) represents the melting of (X)*n*·(U)*n*, the T_m of which has been lowered 5 °C since the (U)*n*·(X)*n* complex is destabilized by the simultaneous drive to form the (A)*n*·(U)*n*·(X)*n* triplex (or the (A)*n*·2(X)*n* triplex). Thus the following reaction accounts for the second break in the 20 °C (A)*n*·(U)*n* + (X)*n* mixing curve:

$$(A)n\cdot(U)n + 2(X)n \rightarrow (A)n\cdot(X)n + (X)n\cdot(U)n$$

Consistent with the above interpretation of melting behavior was the behavior of the (A)*n*·(U)*n*/2(X)*n* mixture to degradation by pancreatic RNase. Using [5-^{3}H]-(U)*n* in the (A)*n*·(U)*n*, the reaction product was just as resistant to RNase as (A)*n*·(U)*n*·(X)*n* itself (data not shown). Note that the RNase incubation conditions correspond to the T_m for the first transition of the melting profile (Figure 4).

Conclusion

Evidence presented herein leads to the conclusion that (X)*n* abolishes the interferon inducing ability of (A)*n*·(U)*n* due to the interaction of one polynucleotide with another to give the (A)*n*·(X)*n*·(U)*n* triplex. Thus (X)*n* joins a group of other polynucleotides that can prevent interferon induction by a specific interaction with the inducing molecule: e.g., (I)*n* by formation of the (A)*n*·(U)*n*·(I)*n* triplex (De Clercq et al., 1975b); (U)*n* and various analogues of (U)*n* by formation of triple helices of the (A)*n*·2(U)*n* class (Torrence et al., 1976). A second class of the inhibition of interferon induction has been defined: that is, the ability of certain polymers [e.g., poly(7-deazaadenylic acid)] to nonspecifically inhibit induction by both (I)*n*·(C)*n* or (A)*n*·(U)*n* by virtue of their antimetabolic activities (De Clercq et al., 1975a). Inspection of Table I suggests that a third class of polynucleotide inhibitors of interferon induction may exist. For instance, the duplexes (U)*n*·(X)*n* and (A)*n*·(X)*n*, although inactive themselves, completely abolish the interferon-inducing capacity of (A)*n*·(U)*n*. They also lead to significant, albeit less dramatic, inhibition of interferon production by (I)*n*·(C)*n*. This phenomenon has been observed previously with other duplexes that themselves are not active inducers (De Clercq et al., 1974). Johnston et al. (1976) have observed that single-stranded polynucleotides and even NaCl, when incubated on the cells at 4 °C, can inhibit induction by (I)*n*·(C)*n*. The basis (or bases) for the third class of inhibition has not yet been resolved, but it seems possible that these phenomena may provide an approach to understanding the initial cellular events involved in interferon induction.

Acknowledgments

We thank Mrs. A. Van Lierde and Mrs. M. Stuyck for excellent technical assistance.

References

Blake, R. D., Massoulié, J., and Fresco, J. R. (1967), *J. Mol. Biol. 30,* 241–308.

De Clercq, E. (1974), *Top. Curr. Chem. 52,* 173–208.

De Clercq, E., Billiau, A., Torrence, P. F., Waters, J. A., and Witkop, B. (1975a), *Biochem. Pharmacol. 24,* 2233–2238.

De Clercq, E., and Merigan, T. C. (1969), *Nature (London) 222,* 1148–1152.

De Clercq, E., Torrence, P. F., De Somer, P., and Witkop, B. (1975b), *J. Biol. Chem. 250,* 2521–2531.

De Clercq, E., Torrence, P. F., and Witkop, B. (1974), *Proc. Natl. Acad. Sci. U.S.A. 71,* 182–186.

De Clercq, E., Torrence, P. F., and Witkop, B. (1976), *Biochemistry 15,* 717–724.

Fikus, M., and Shugar, D. (1969), *Biochim. Biophys. Acta 149,* 107–126.

Johnston, M. D., Atherton, K. T., Hutchinson, D. W., and Burke, D. C. (1976), *Biochim. Biophys. Acta 435,* 69–75.

Michelson, A. M., and Monny, C. (1966), *Biochim. Biophys. Acta 124,* 460–474.

Sigler, R. B., Davies, D. R., and Miles, H. T. (1962), *J. Mol. Biol. 5,* 509–517.

Torrence, P. F., De Clercq, E., and Witkop, B. (1976), *Biochemistry 15,* 724–734.

Torrence, P. F., De Clercq, E., and Witkop, B. (1977), *Biochim. Biophys. Acta* (in press).